



Original Article

Some Preliminary Results of the Synthesis and Investigation of the Glass/FTO/Si/Au/ Embedded Thin Film for Application in the Modified Plasmonic Solar Cell

Nguyen Tien Thanh^{3,2}, Dao Khac An^{1,2,*}, Nguyen Si Hieu², Nguyen Thi Mai Huong⁴

¹*Institute of Theoretical and Applied Research (ITAR), Duy Tan University, Hanoi, Vietnam*

²*Institute of Materials Science, Vietnam Academy of Science and Technology (VAST),
18 Hoang Quoc Viet, Hanoi, Vietnam*

³*Graduate University of Science and Technology, VAST, 18 Hoang Quoc Viet, Hanoi, Vietnam*

⁴*Institute of Applied Physics and Scientific Instruments, VAST, 18 Hoang Quoc Viet, Hanoi, Vietnam*

Received 03 August 2020

Revised 27 October 2020; Accepted 15 November 2020

Abstract: This paper outlines the synthesis of the glass/FTO/Au/ and of the glass/FTO/Si/Au/ multilayers and some obtained experimental results. Based on the measured results we observed that the structure of the sputtered Si layer is an amorphous phase meanwhile the structure of the sputtered Au layer is a crystallized phase. Depending on the sputtered layers (Si, Au) thicknesses and thermal annealing conditions the different surface morphologies of the Au layer with different sizes of clusters are formed on both the FTO and Si layers. Notably, the optical absorption spectra of the glass/FTO/Si/Au film in both cases of thermal annealing and without thermal annealing are significantly enhanced in comparison with the optical absorption spectra of the glass/FTO/Au film. These enhanced optical absorptions are explained by the absorption role of the amorphous Si film and/or the amorphous Si/Au Schottky layers/nanoparticles barrier configurations caused. The glass/FTO/Si/Au layer/nanoparticles thin films could be used for integration with the core structure (Au/TiO₂) of plasmonic solar cell to form the modified plasmonic solar cells for aiming to enhance the solar cell performance.

Keywords: glass/FTO/Au multilayers, glass/FTO/Si/Au multilayers; amorphous Si layer; Au nanoparticles /cluster; photo absorption enhancement.

*Corresponding author.

Email address: daokhacan@duytan.edu.vn

<https://doi.org/10.25073/2588-1124/vnumap.4589>

1. Introduction

Recently the energy security problem is one of the biggest challenges for mankind to face and solve. Scientists have to extensively focus on researches for using solar energy in the forms of thermal and electrical energy. So far there are four solar cell generations that have been developing, among them the Dye-Sensitive Solar Cell (DSSC) including the plasmonic solar cell (PSC) belonging to the thin films solar cells generation, which are very interested. The operating principle of DSSC and PSC can be distinguished in more detail in the works [1, 2]. In 1991, Brian O'Regan and Michael Grätzel [1] published firstly the paper in the Nature journal of a low-cost, high-efficiency solar cell based on dye-sensitized colloidal TiO_2 films, so-called DSSC [1]. The DSSC is operating on the base of a suitable semiconductor formed between a photo-sensitized anode and a cell electrolyte, a photoelectrochemical system. In contrast to the conventional solar cell system, here the light radiation is absorbed by a sensitizer, which is anchored to the surface of a wideband semiconductor then separated to the electrodes generating electrical current, meanwhile, the PSC is the use of scattering from metal nanoparticles (MNPs) excited at their surface Plasmon resonance with manipulation of electromagnetic signals by coherent coupling of photons to free electron oscillations at the interface between a conductor and a dielectric to form the localized surface plasmon resonances (LSPRs), this phenomenon is observed mainly in MNPs/semiconductor, for example in Au (Ag)/ TiO_2 (ZnO) and the PSC operation depends strongly on the size and shape of the nanoparticles (NPs) [1-4]. So far, many problems concerning the DSSC and PSC have been intensively studying. Each component in the DSSC (Dyes, semiconductor type, electrolyte, photoconductor, electrodes) and in PSC (MNPs, solid state dye- sensitizer, semiconductor quantum dots, high band gap semiconductors (TiO_2 , ZnO,...)) has been developing both in manufacturing methods as well as searching new substitution materials for production of the different DSSCs and PSCs with the aims to produce the higher efficiency, larger area, low cost, stable operation, long life [2-13]. In order to increase the performance of DSSCs and PSCs, the scientists have been developing and integrating different additional layers into the initial core structures of DSSC and PSC [5-10]. Here it is worth noting that there is a very interesting research orientation that is the integration of the different structures of Si materials (Si substrate, Si thin film, amorphous silicon (a-Si), Hydrogenated amorphous silicon (a-Si:H) and SiO_2 layers) into the initial PSCs to form so called the modified PSCs such as the Surface Plasmon enhanced silicon solar cells, Au-Si plasmonic platforms [14-17]. Although so, the ideal concerning the research work of the integration of the a-Si/Au NPs Schottky barriers structure into the core Au/ TiO_2 plasmonic structure to form the modified PSCs has not been studying more in detail.

This paper outlines the technological process for the synthesis of two groups: the glass/FTO/Au (FA group) and the glass/FTO/Si/Au/ multilayers configurations (SA group) using sputtering technology for deposition of Si layer onto the surface of the FTO/glass substrates and then deposition of Au layers with different thicknesses, after that a samples group are thermally annealed at 350°C for 30 minutes in the low vacuum (10^{-1} torr) to form the a-Si/Au NPs embedded configurations, the rest samples group are without thermal annealing remaining the a-Si/Au multilayers configurations. Their properties of the surface morphologies, their structural and chemical compositional properties as well as the optical absorptions have been investigated, showed and discussed in the comparison between two sample groups based on the measured results of SEM, EDX, XRD and optical absorptions spectra. The application ability of the glass/FTO/Si/Au NPs embedded thin film configuration for integrating into the conventional Au/ TiO_2 core plasmonic structure to form, so called the modified PSCs will also be discussed.

2. Materials and methods

Materials used in our experiments are fluorine doped tin oxide coated on a glass slide (glass/FTO) which has the sheet resistivity is about $\sim 7 \Omega/\text{square}$ (from Aldrich Inc). Samples are divided into two groups: in the first group, Au layers are sputtered onto the glass/FTO substrate directly with the sputtered times are 10 s, 20 s, 30 s and 40 s, the obtained Au layer thicknesses are 30 nm, 60 nm, 90 nm and 120 nm, respectively; in the second group, the Si layers are sputtered onto the glass/FTO substrate, following the Au layers are sputtered with the same sputtering times and layers thicknesses obtained as in above mentioned. The sputtering conditions occurred in 0.5 Pa pressure and 50 W power conditions. The samples' labels, technological conditions and their features can be seen in Table 1.

Table 1. Samples labels, the Au sputtered times and Au layers thicknesses obtained on the glass/FTO/Au and glass/FTO/Si (~ 200 nm)/Au thin films

Sample's configuration	Glass/FTO/Au/ samples (FA group)				Glass/FTO/Si(~ 200 nm and ~ 500 nm)/Au/ samples (SA group)			
	FA-10	FA-20	FA-30	FA-40	SA-10	SA-20	SA-30	SA-40
Samples' labels	FA-10	FA-20	FA-30	FA-40	SA-10	SA-20	SA-30	SA-40
Sputtering time of Au	10 s	20 s	30 s	40 s	10 s	20 s	30 s	40 s
The Au layer thickness	30 nm	60 nm	90 nm	120 nm	30 nm	60 nm	90 nm	120 nm

After that, one group was thermally annealed at 350°C for 30 min in the low vacuum (10^{-1} torr) condition; another group was not thermally annealed. The synthesized samples were investigated by SEM, EDX, XRD techniques and measured the photo absorption spectra on the UV-VIS spectroscopy. Figure 1 shows the draft structural scheme of the modified PSC expected after integration where there is so called the *front layer* that is glass/FTO/Si/Au/ nanoparticles embedded thin film that is belonging to the investigating survey in this paper.

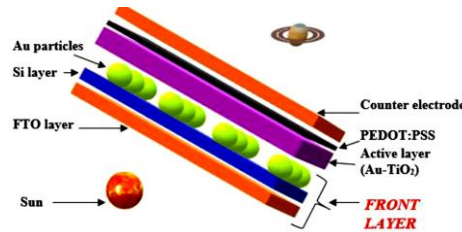


Figure 1. The draft structure scheme of the modified plasmonic solar cell expected to do where the front layer of glass/FTO/Si/Au nanoparticles embedded thin film will be synthesized and investigated

3. Results and Discussion

3.1. The Surface Morphology and the Au Nanoparticles-clusters Formation on the Glass/FTO/Au/ and glass/FTO/Si/Au/ Embedded Thin Films

In order to use the photo effect of the sputtered Si/Au NPs Schottky barriers configurations for aiming integration with the Au/TiO₂ core structural plasmonic solar cell as expected, the FA and SA samples have to thermally annealed at certain conditions to form Au NPs on the Si layer, and then investigate the Au NPs - clusters formation at different Au layers thicknesses.

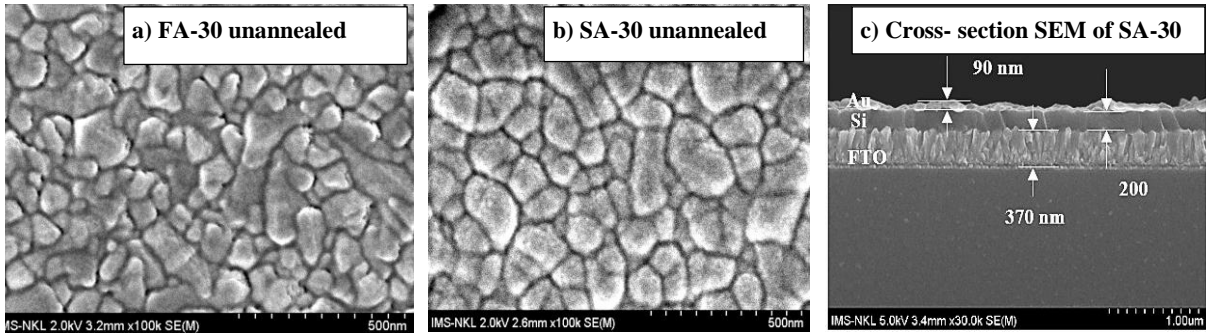


Figure 2. SEM micrographs of the top view surface morphologies of FA-30 sample without annealing (a); and of SA-30 sample without thermal annealing (b); the cross-section SEM image of SA-30 (c)

Figure 2a,b show SEM images of the surface morphologies of the FA-30 and SA-30 samples without thermal annealing where the Au (90 nm) layers are being on different thin films of FTO and Si. The top view surface situations here are fine flats without any Au droplets-clusters formed. The grain sizes of the FTO layer being on FTO/glass (FA-30) thin film (Figure 2a) and the grain sizes of the sputtered Si layer being on Si/FTO/glass (SA-30) thin film (Figure 2b) are shown very clearly. Figure 2c shows the cross-section SEM of SA-30 sample, as an example, with the sizes of the thicknesses of the different layers where from the top to the bottom: Au layer thickness is about 90 nm, Si layer thickness is about 200 nm, the FTO layer thickness is about 370 nm and the next to FTO layer is glass layer.

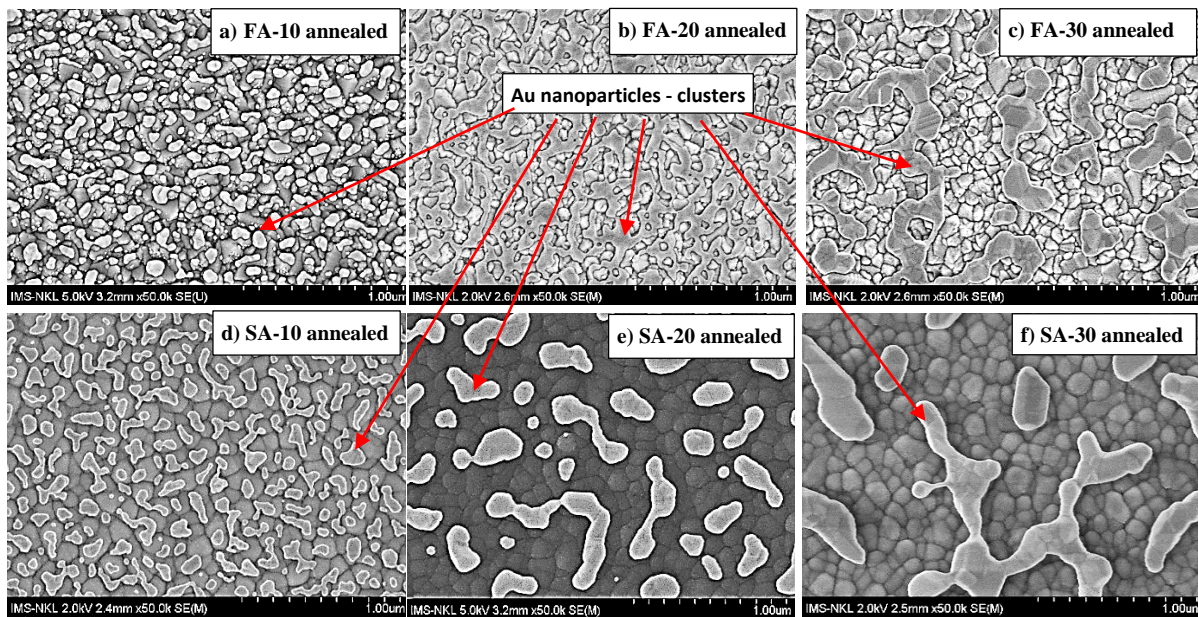


Figure 3. The SEM images of the different FA (a,b,c) and SA (d, e, f) group after thermal annealing on 350 °C for 30 min in low vacuum.

Figure 3 shows the surface morphologies of FA and SA samples group together with the Au NPs or clusters formed after thermal annealing at 350 °C temperature for 30 mins in low vacuum (10^{-1} torr) conditions. The results showed very clearly that the shape and size of Au NPs or clusters are different from each other sample depending on the thickness of the sputtered Au layers and the type of substrate.

Notably, in the case of 10 s sputtering time with 30 nm Au layer thickness, the Au NPs formed with the size of about 20 - 40 nm (Figure 3a,d), while for the cases of the thicker Au layer thicknesses (60 nm and 90 nm Au layers) the bigger Au NPs or clusters were formed on samples surface, their sizes are in the range of about from 40 nm - 150 nm (Figure 3b,e,c,f), the sizes and forms of the Au NPs (smaller than 100 nm) or clusters (bigger than 100 nm) are also formed differently on the FTO/glass and Si/FTO/glass surfaces.

We see that the Au NPs are mainly formed in the case of the thin 30 nm Au layer thickness for FA-10 and SA-10 samples (Figure 3a,d). These results confirmed also the statement of Anna Gapska et al. [17] the formation of gold nanostructures on silicon can start below the eutectic temperature. Here two processes could be considered in explaining the formation of nanostructures: dewetting and directional solidification of a eutectic [17]. In addition, in the gold–silicon system, with the thicker Au layers, as in this case, an Au-rich near eutectic phase could be considered at a near eutectic temperature of 363 °C

At this temperature, because the solubility of Au in Si is negligible, the Au–Si near eutectic phase does not wet the Si surface. Consequently, Si/Au NPs/droplets do not dissolve on the Si surface, forming the nanostructures during cooling. Unfortunately, it is not possible to clearly determine what type of dewetting (heterogeneous and/or spinodal) occurs for the studied samples so the consideration and explanation here are therefore is only qualitative. We also observed that when the thickness of the sputtered Au layer increased to 60 nm and 90 nm then the formed sizes of Au NPs/droplets after thermal annealing increased, their forms are also changed to larger, more elongated, and also more irregular as the mass thickness of Au is increased as in Figure 3b,e and Figure 3c,f. Here it is worth noting that the Au NPs/ clusters formed on the sputtered Si layer with different sizes (see on Figure 3) can be considered to form many Si/Au NPs Schottky barriers contacts due to Au NPs did not dissolve on the Si surface [8, 17]. Figures 4 show the sizes distribution of the Au nanoparticles or clusters estimated by the Gwyddion roughness tool when analyzing the SEM images, these results are only qualitative values.

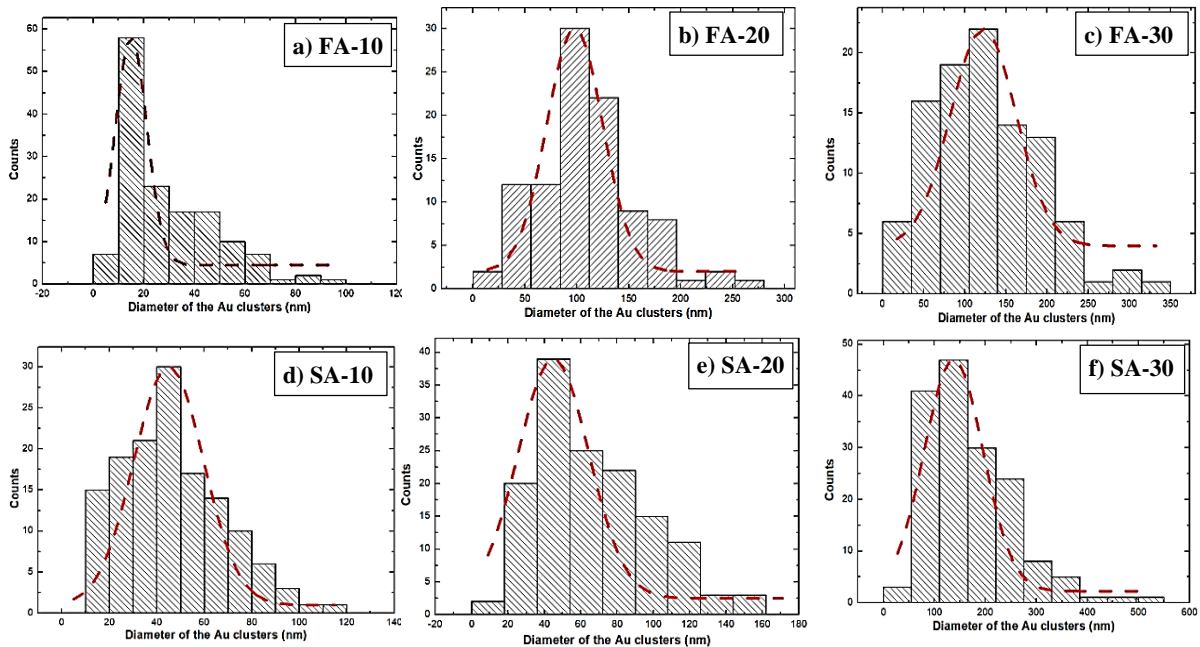


Figure 4. The sizes distribution of the Au nanoparticles or clusters on glass/FTO surface (a, b, c), and on the glass/FTO/Si surface (d, e, f).

3.2. The Structural Property and Chemical Composition of the Glass/FTO/Au and glass/FTO/Si/Au Multilayers Thin Films before and after Thermal Annealing

Figure 5(a) shows X-ray diffraction spectra (XRD) of the SA-30 samples before and after annealing. We observed that after thermal annealing the several XRD peaks have increased higher and their widths of peaks have changed due to the layers have recrystallized and better quality of layers formed after thermal annealing. The diffraction peaks of Si were not observed in the spectrum, this result can be explained by the existence of the *amorphous Si (a-Si)* structure, and this means that the Si crystal structure is not yet formed during the thermal annealing at 350 °C. There are two peaks concerning the metallic gold where the Au had crystal structure that detected by the diffraction peaks at 2-theta positions of 38° and 44.5° corresponding to (111) and (200) lattice planes, respectively. The rest other peaks belong to the diffraction peaks of the FTO substrate.

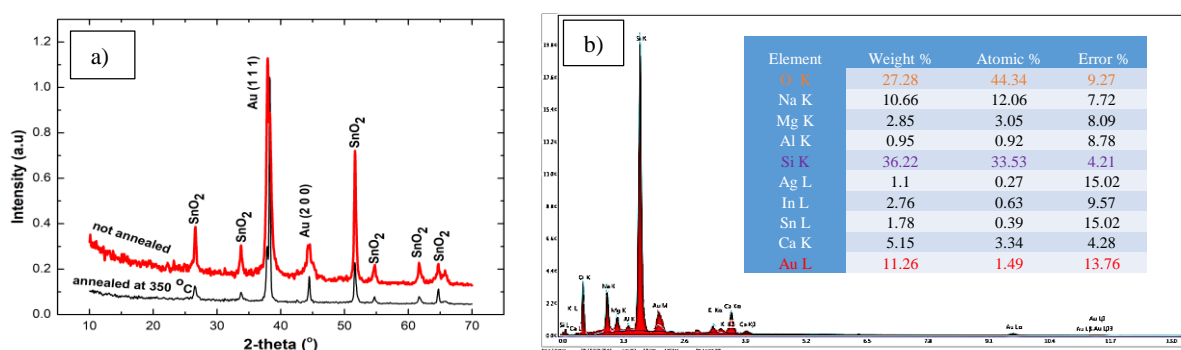


Figure 5. (a) X-ray diffraction spectra of the SA-30 sample for the case of sample without annealing (red color) and after annealing (black color). (b) EDX measurement results of the SA-30 sample after annealing.

The chemical compositions can be seen from the EDX measured results for the glass/FTO/Si/Au (SA-30) after thermal annealing in Figure 5 (b). Although the Si peaks have not found in XRD spectrum but in the EDX measured results we see that all elements compositions of Oxygen (O), Si, and Au and of the glass/FTO are presented. The Si composition here is 36.22% weight and 33.53% atomic. The Au composition is 11.26% weight and 1.49% atomic. The rest compositions are belonging to the glass/FTO substrate.

3.3. Absorption spectra of the glass/FTO/Au and glass/FTO/Si/Au embedded thin films before and after thermal annealing

The optical absorption spectra of two FA and SA samples groups before and after thermal annealing have measured on the UV-VIS spectroscopy. Here it is worth noting that the glass/FTO substrates used in our experiment samples have the same features. The transmission of glass is 90% and of FTO is 80-85% in the wavelength region from 300-1100 nm. These films have strong absorption at wavelength below 300 nm [18]. So the different obtained results of absorption spectra in different samples are caused by the different features of the sputtered Au and Si layers as well as technological conditions. Our obtained results of absorption spectra sometimes are different due to the effect of interference phenomenon arisen at multilayers thin film. Here we show two typical results of photo absorptions for the glass/FTO/Si/Au thin films (SA samples) in comparison with that of the thin films without the sputtered Si layers (FA samples).

Figure 6 shows the photo absorption spectra of two kinds of sample groups: (a) FA-10, SA-10 and (b) FA-40, SA-40 samples (See Table 1). As Figure 6 shows three kinds of absorptions for three different samples: i) the absorption of the glass/FTO/Au samples (black color curve), these curves have a slight wavy form, it may be due to the effect of interference phenomenon in multilayers configuration; ii) the absorption of the glass/FTO/Si/Au samples without thermal annealing (red color curves) where the red solid curves are the measured curves which have the sine oscillation form, whereas the red dashed lines are averaged drawn curves. We observed that the red averaged absorption curves enhanced in the whole spectrum range of wavelength in comparison with the glass/FTO/Au samples (black color curves), especially strongly enhanced in the short wavelength from 400 nm to 600 nm; *in this case the absorption enhancement, we think, could explain by the photo absorption role of Au thin film layer on the a-Si layer forming the Schottky barrier configuration via the surface interactions between the Au layer and a-Si layer*; iii) the photo absorption of the glass/FTO/Si/Au samples with thermal annealing (blue curves) where the blue color solid curves are the measured curve, they have also the sine oscillation form meanwhile the blue dashed lines curves are averaged drawn curve. Here we observed also that the blue absorption curves (measured curves and averaged drawn curves) strongly enhanced with high absorption values, notably the absorption curves were shifted to the left due to the Au NPs absorption dominated in the visible spectrum wavelength [17] in comparison with the red absorption curves of the glass/FTO/Si/Au samples without thermal annealing. Here we think that the absorptions of the different Au NPs and the surface interplaying interactions between the Au NPs and a-Si forming the a-Si/Au NPs Schottky barrier configurations which play important role in photo absorption enhancement.

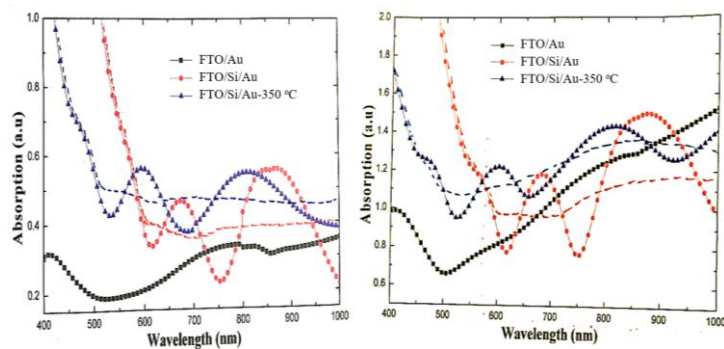


Figure 6. The photo absorption spectra of FA-10, SA-10 samples (a), and of FA-40, SA-40 samples (b) with and without annealing in comparison in Fig. 6a, b) where: i) the black color curves for the FA-10 and FA-40 samples with 30 nm and 120 nm Au layers, respectively; ii) the red color curves for the case of without thermal annealing (solid curves are the measured curves, the dashed lines curves are the averaged drawn curves) for the SA-10 and SA-40) samples of glass/FTO/Si (~200 nm)/Au with 30 nm and 120 nm Au layers, respectively; iii) the blue color curves (solid curves are the measured curves, the dashed lines curves are the averaged drawn curves) for the SA-10 and SA-40 samples of the glass/FTO/Si (~200 nm)/Au in the case of thermal annealing. In the case of FA-10 sample in Figure 6a), the absorptions values are small that varied in the low narrow range of from 0.2 to 0.4 value in the absorption vertical axis, meanwhile in the case of FA-40 sample in Figure 6b) the absorptions values are larger that varied in the wider range of from 0.7 to 1.5 value for whole the wavelength range.

Here it is worth noting that in the absorption measurements, the incident light beam came firstly to the glass going through the sample then the light beam comes out from the Au layer to get minimum reflecting-scattering. The forms of the photo absorption curves in the presence of the Si layer have strong sine oscillation forms as shown (Figure 6). This result can be explained by the interference phenomenon between the incoming and reflecting radiations during measuring photo absorption on the glass/FTO/Si/Au layer and/or the glass/FTO/Si/Au NPs multilayers configurations. The wavy nature in

the glass/FTO/Si/Au multilayers film could be formed based on the equation $2nd = m\lambda$ (where n is the refractive index, d is the thickness of the film, m is the interference number, λ is the interference wavelength). This effect could be occurred due to the refractive index of the a-Si/Au film is low [18].

4. Conclusion

We have developed the technological process for synthesizing the glass/FTO/Au/ and glass/FTO/Si/Au/ thin films with different Au layer thicknesses from 30 nm to 120 nm. Depending on the technological conditions (with and without thermal annealing) and Au layers thicknesses, the different surface morphologies of the Au flat surface layer or the Au bumpy surface layer with different sizes of NPs/clusters are formed on both the samples surfaces of FTO and amorphous Si layers.

We have investigated the surface morphologies, structural and photo absorption properties of both the glass/FTO/Au/ and glass/FTO/Si/Au/ samples with and without thermal annealing in comparison with each other based on the investigated results of SEM, XRD, EDX and UV-VIS spectroscopy techniques. The obtained experimental results showed that the sizes of Au NPs formed on the thin films are in the range of from 30 nm to 150 nm, the sputtered Si layer has an amorphous structural phase, the sputtered Au layer has the crystal structure with two the diffraction peaks at 2-theta positions of 38° and 44.5° corresponding to (111) and (200) lattice planes.

In the presence of the Au thin film layer (in the case without thermal annealing) being on the sputtered Si layer has absorption coefficient in the range of near IR region, the absorption curve enhanced in whole spectrum range of wavelength, especially strongly enhanced in the short wavelength from 400 nm to 600 nm; *this could explain by the photo absorption role of the configuration of Au thin film/ a-Si layer forming the Schottky barrier configuration via the surface interactions between the Au layer and a-Si layer, while* in the presence of the Au NPs (in the case with thermal annealing) being on the a-Si layer, the absorption curve also enhanced in whole spectrum range and in the short wavelength from 400 nm to 600 nm; *this could explain by the photo absorption role of the configuration of Au NPs/a-Si layer forming the Schottky barriers configurations via the surface plasmon resonance as well as the surface interactions between the Au NPs and a-Si layer forming the Schottky barriers configurations. However, from the variations of the photo absorptions curves are similar trends in the two cases of with and without thermal annealing for the thicker a-Si layers, we can conclude that the photo absorption of a-Si layer plays a very important role in the glass/FTO/Si/Au multilayers configuration.*

The measured photo absorption spectra have wave oscillation form. This phenomenon could be explained by the interference phenomenon between the incoming and reflecting photo radiations on the glass/FTO/Si/Au multilayers sample based on the equation $2nd = m\lambda$

These obtained absorption enhancement results have significant meanings in an application for integrating the glass/FTO/Si/Au nanoparticles embedded thin films into the conventional Au/TiO₂ core structural PSCs to form the modified PSC with the aims to enhance the modified PSC's performance including the photo absorption and collection efficiency. These problems will be discussed in the forthcoming paper.

Acknowledgments

This research is funded by the Vietnam National Foundation for Science and Technology Development (NAFOSTED) under grant number 103.02-2017.346. The authors would like to express

our sincere thanks to the Institute of Materials Science (IMS), Vietnam Academy of Science and Technology (VAST) for their supports and encouragements.

References

- [1] Brian O'Regan and Michael Grätzel; a low-cost, high-efficiency solar cell based on dye-sensitized colloidal TiO₂ films, *Nature*, 353 (1991) p. 6346
- [2] A.Hema Chander , M.Krishna , Y.Srikanth; Comparison of Different types of Solar Cells – a Review, *IOSR-JEEE*, 10 (6), (2015) 151-154. DOI: 10.9790/1676-106115115
- [3] Meidan Ye, Xiaoru Wen, Mengye Wang, James Iocozzia, Nan Zhang, Changjian Lin, and Zhiqun Lin; Recent advances in dye-sensitized solar cells: from photoanodes, sensitizers and electrolytes to counter electrodes, *Mater. Today*, 18 (3) (2014) 155-162. <http://dx.doi.org/10.1016/j.mattod.2014.09.001>
- [4] Xuanhua Li, Wallace C. H. Choy, Lijun Huo, Fengxian Xie, Wei E. I. Sha, Baofu Ding, Xia Guo, Yongfang Li, Jianhui Hou, Jingbi You, and Yang Yang; Dual Plasmonic Nanostructures for High Performance Inverted Organic Solar Cells, *Adv. Mater.*, 14 (22) (2012) 3046-3052. DOI: 10.1002/adma.201200120
- [5] Dixon D. S. Fung, Linfang Qiao, Wallace C. H. Choy, Chuandao Wang, Wei E. I. Sha, Fengxian Xie and Sailing He, Optical and electrical properties of efficiency enhanced polymer solar cells with Au nanoparticles in a PEDOT–PSS layer, *J. Mater. Chem.*, 21 (2011) 16349. DOI: 10.1039/c1jm12820e
- [6] FengXian Xie, Wallace C. H. Choy, Charlie C. D. Wang, Wei E. I. Sha, and Dixon D. S. Fung; Improving the efficiency of polymer solar cells by incorporating gold nanoparticles into all polymer layers, *Appl. Phys. Lett.* 99 (2011) 153304, doi: 10.1063/1.3650707
- [7] M. Ghaffari, M. Burak Cosar, Halil I. Yavuz, M. Ozenbas, Ali K. Okyay; Effect of Au nano-particles on TiO₂ nanorod electrode in dye-sensitized solar cells, *Electrochim. Acta* 76 (2012) 446–452. <http://dx.doi.org/10.1016/j.electacta.2012.05.058>
- [8] Tanujjal Bora, Htet H. Kyaw, Soumik Sarkar, Samir K. Pal and Joydeep Dutta; Highly efficient ZnO/Au Schottky barrier dye-sensitized solar cells: Role of gold nanoparticles on the charge-transfer process, *Beilstein J. Nanotechnol.*, 2 (2011) 681–690. doi:10.3762/bjnano.2.73
- [9] Sawanta S. Mali, Chang Su Shim and Chang Kook Hong; In-Situ processed gold nanoparticle embedded TiO₂ nanofibers enabling plasmonic perovskite solar cells exceeding 14% conversion efficiency, *Nanoscale*, 8(5) (2015) DOI 10.1039/C5NR07395B
- [10] Zelin Lu, Xujie Pan, Yingzhuang Ma, Yu Li, Lingling Zheng, Danfei Zhang, Qi Xu, Zhijian Chen, Shufeng Wang, Bo Qu, Fang Liu, Yidong Huang, Lixin Xiao, and Qihuang Gong; Plasmonic-Enhanced Perovskite Solar Cells Using Alloy Popcorn Nanoparticles, *RSC Adv.*, 5 (2015) 11175-11179. DOI: 10.1039/C4RA16385K
- [11] Xiang-Chao Ma, Ying Dai, Lin Yu and Bai-Biao Huang; Energy transfer in plasmonic photocatalytic composites, *Light Sci Appl* 5 (2016); doi:10.1038/lsa.2016.17
- [12] Vivian E. Ferry, Jeremy N. Munday, and Harry A. Atwater; Design Considerations for Plasmonic Photovoltaics, *Adv. Mater.*, 22 (2010) 4794–4808
- [13] Yoon Hee Jang, Yu Jin Jang, Seokhyoung Kim, Li Na Quan, Kyungwha Chung, and Dong Ha Kim; Plasmonic Solar Cells: From Rational Design to Mechanism Overview, *Chem. Rev.*, 116 (2016) 14982–15034
- [14] Vipinraj Sugathan , Elsa John, K. Sudhakar; Recent improvements in dye sensitized solar cells: A review ; *Renew. Sustain. Energy Rev.*, 64 (2015) 5254. <http://dx.doi.org/10.1016/j.rser.2015.07.076>
- [15] P. Mandal, S. Sharma; Progress in plasmonic solar cell efficiency improvement: A status review, *Renew. Sustain. Energy Rev.*, 65 (2016) 537–552
- [16] S. Pillai, K. R. Catchpole, T. Trupke, and M. A. Green; Surface plasmon enhanced silicon solar cells (ARC Photovoltaics Centre of Excellence, University of New South Wales, Sydney, Australia 2052; *J. Appl. Phys.*, 101 (2007) 093105
- [17] Anna Gapska, Marcin Lapiński, Paweł Syty, Wojciech Sadowski, Józef E. Sienkiewicz and Barbara Kościeliska; Au–Si plasmonic platforms: synthesis, structure and FDTD simulations; *Beilstein J. Nanotechnol.*, 9 (2018) 2599–2608
- [18] Jun Wang, Qianwen Ran, Xunhu Xu, Binghua Zhu and Wenjuan Zhang; Preparation and Optical Properties of TiO₂-SiO₂ thin films by Sol-gel Dipping Method, *IOP Conf. Ser.: Earth Environ. Sci.* 310 (2019) 042029. doi:10.1088/1755-1315/310/4/042029